Cell

# Spinophilin Facilitates Dephosphorylation of Doublecortin by PP1 to Mediate Microtubule Bundling at the Axonal Wrist

Stephanie L. Bielas,[1,2] Finley F. Serneo,[2] Magdalena Chechlacz,[2] Thomas J. Deerinck,[3] Guy A. Perkins,[3] Patrick B. Allen,[4] Mark H. Ellisman,[3] and Joseph G. Gleeson[2,*]
[1] Neurobiology Section, Division of Biological Sciences
[2] Laboratory for Neurogenetics, Department of Neurosciences
[3] National Center for Microscopy and Imaging Research
University of California, San Diego, La Jolla, CA 92093, USA
[4] Department of Psychiatry, Yale University School of Medicine, New Haven, CT 06508, USA
*Correspondence: jogleeson@ucsd.edu
DOI 10.1016/j.cell.2007.03.023

## SUMMARY

The axonal shafts of neurons contain bundled microtubules, whereas extending growth cones contain unbundled microtubule filaments, suggesting that localized activation of microtubule-associated proteins (MAP) at the transition zone may bundle these filaments during axonal growth. Dephosphorylation is thought to lead to MAP activation, but specific molecular pathways have remained elusive. We find that Spinophilin, a Protein-phosphatase 1 (PP1) targeting protein, is responsible for the dephosphorylation of the MAP Doublecortin (Dcx) Ser 297 selectively at the "wrist" of growing axons, leading to activation. Loss of activity at the "wrist" is evident as an impaired microtubule cytoskeleton along the shaft. These findings suggest that spatially restricted adaptor-specific MAP reactivation through dephosphorylation is important in organization of the neuronal cytoskeleton.

## INTRODUCTION

Growth cone features that are distinctive from those of the axon shaft were noted first by Cajal (Ramón y Cajal, 1988). The growth cone is the motile end of the axon, is enriched in dynamic actin and microtubule (MT) components, and determines the direction of axonal growth. It has been divided into three regions: the peripheral domain containing a dense meshwork of actin forming lamellipodia and filopodia, the transition domain where actin filaments anchor into a loose MT network, and the central domain containing splayed MTs and organelles of varying size (Dent and Gertler, 2003). Between the central domain and the axonal shaft is a region surrounded by actin where splayed MTs become bundled into dense parallel arrays (Dehmelt and Halpain, 2004) that we refer to as the neuronal "wrist". Defects in the "wrist" domain would therefore be predicted to result in defects in the organization of the MT cytoskeleton in the axonal shaft. The molecules that function at these transition zones have not yet been clearly defined.

Among the candidates for mediating MT bundling is Doublecortin (Dcx), a MAP with a role in MT stabilization and bundling that has been localized to the growth cone (Friocourt et al., 2003). Dcx was initially identified as the causative gene for the human neuronal migration disorder double cortex and X-linked lissencephaly (des Portes et al., 1998), and is expressed by postmitotic neurons. It consists of an N-terminal repeated tubulin binding domain (R1 and R2) and a C-terminal serine-proline rich domain. Deletion in mouse results in excessively branched axonal shafts in migrating neurons (Kappeler et al., 2006; Koizumi et al., 2006a), suggesting Dcx may be required for formation of stable MT.

Recent data has highlighted the important role that Dcx phosphorylation plays in mediating MT interactions (Gdalyahu et al., 2004; Schaar et al., 2004; Tanaka et al., 2004b). One kinase responsible for Dcx phosphorylation is cyclin-dependent kinase 5 (Cdk5), a Serine/Threonine (S/T) kinase primarily active in terminally differentiated neurons (Ohshima et al., 1996). Cdk5 phosphorylation of Dcx at serine 297 reduces its affinity for MTs and its ability to polymerize tubulin (Tanaka et al., 2004b). The dynamic nature of cytoskeletal reorganization underlying neurite outgrowth and migration predicts that Dcx phosphorylation, like that of other MAPs, is tightly regulated by both kinases and phosphatases. However, unlike tyrosine kinases and phosphatases that are represented in the mammalian genome in comparable numbers, the quantity of S/T kinases far exceeds that of S/T phosphatases (Ceulemans and Bollen, 2004). Thus, phosphatase diversity only matches that of the kinases when the number of phosphatase regulators is considered. Much of the data concerning the role of S/T phosphatases for MAPs is

based on results of pharmacological studies and thus potential adaptor molecules that may regulate these interactions have not been identified.

One such potential adaptor molecule with which Dcx has been shown to interact is Spinophilin (Spn), an actin binding protein with an established role in subcellular targeting of Protein phosphatase 1 (PP1), an S/T phosphatase that controls many aspects of cellular physiology (Allen et al., 1997). Spn is able to bind and bundle F-actin, which is theorized to be important for regulating spine morphology (Satoh et al., 1998). Consistent with these observations, *Spn*$^{-/-}$ mice exhibit abnormal spine number and formation (Feng et al., 2000). Here, we tested the hypothesis that Spn may function as an adaptor molecule for PP1 to regulate the MAP activity of Dcx.

## RESULTS

### Impaired Axon Outgrowth in *Dcx* Mutant Brains

Corpus callosal hypoplasia is apparent in the MRIs of human males with *DCX* mutations (Figure 1A). Additionally, published data indicates that Dcx expression is upregulated in corpus callosal (CC) projection neurons during periods of axonal growth in mice (Arlotta et al., 2005), together suggesting a potential role in axonal extension and/or stabilization. We therefore tested *Dcx*$^{-/y}$ mice for alterations in axonal outgrowth by DiI labeling projections when axons are extending in multiple regions of the brain. Injection into the medial subcortical zone at E14.5 labeled cortico-thalamic (CT) axons that extended to the cortico-striatal (CS) boundary in wild-type (WT) mice (Figure 1B). In *Dcx*$^{-/y}$ mice, however, none of the labeled axons reached the CS boundary. By E15.5 these CT axons had extended into the region of the striatum and thalamus in WT mice, whereas only a fraction of these axons had reached the CT boundary in *Dcx*$^{-/y}$ mice, and even fewer had reached the striatum and thalamus (Figures 1C and 1D). By E16.5, these defects became less apparent, while the corpus callosal axonal tract, which typically reaches the medial extent of the telencephalon by this time, showed a defect in axonal length (Figure 1E). This effect on outgrowth did not appear to be secondary to impaired neuronal migration, because *Dcx* knockout mice do not display discernable defects in the positioning of neurons (Corbo et al., 2002; Kappeler et al., 2006). Although by the time of birth, these developmental delays had not resulted in clear morphological defects, these findings suggest a requirement for *Dcx* in timing of axonal outgrowth.

### Dcx/Spn/PP1 Localization at the Wrist Suggests Possible Involvement in Axonal Outgrowth

It had been shown that Dcx interacts with the PP1-adaptor protein Spn, a multidomain protein with N-terminal actin binding, PSD-95/Dig/ZO-1 homology (PDZ) and coiled-coil (CC) domains (Tsukada et al., 2003), and our own work confirmed these results (Figures S1 and S2 in the Supplemental Data available with this article online). To determine if this interaction might play a role in the *Dcx*$^{-/y}$

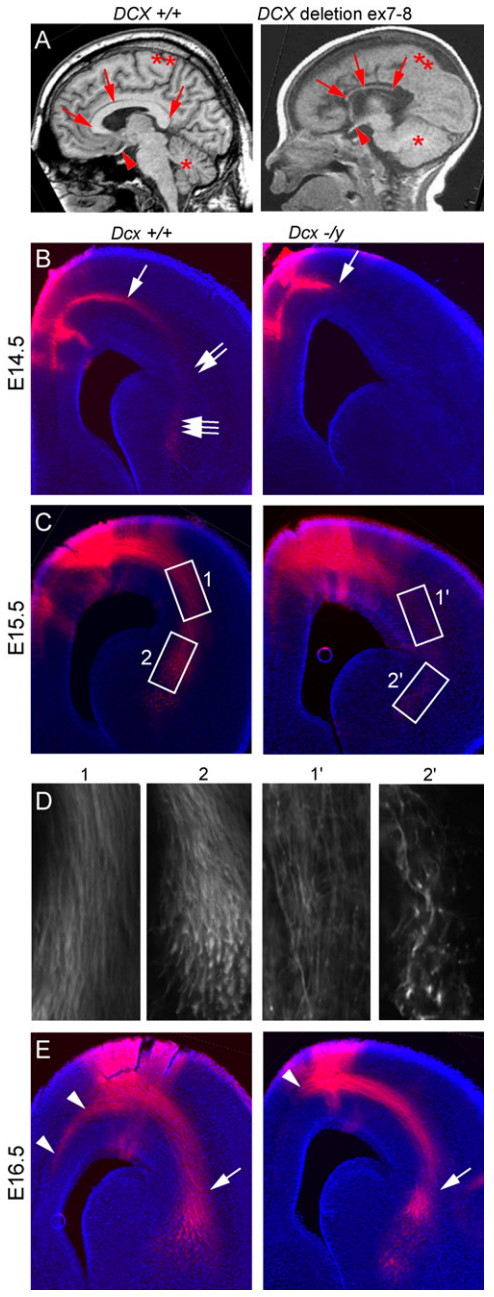


**Figure 1. Delayed Axonal Extension in *Dcx*$^{-/y}$ Brains**

(A) Midline sagittal T1-weighted brain MRI from normal showed well-formed CC and a male with deletion of *DCX* exon 7-8 showed severe CC hypoplasia (arrows). Optic nerve (arrowhead), cerebellum (*), cortex (**).

(B) E14.5 DiI injected into medial subcortical region showed extensive fibers in subcortical white matter (arrow), cortico-striatal (CS) boundary (double arrows) and striatal-thalamus region (triple arrows). Mutant showed minimal axonal extension from the injection.

(C) E15.5 DiI injection showed labeling of corticothalamic (CT) axons at CS boundary (box 1) and striatal-thalamus region (box 2), whereas mutant showed diminished labeling.

(D) High-power views.

(E) E16.5 DiI injection showed diminished axon extension of the CC tract (arrowhead) in mutant. There was some catch-up extension of CT tract by this age (arrow).

axon growth phenotype, we assessed protein localization in cultured cortical neurons at 1 day in vitro (DIV). At this stage, neurites have a well-defined shaft capped by a growth cone, but axonal/dendritic differentiation has not yet occurred. Spn exhibited an unexpected highly distribution at the transition zone between the growth cone and axonal shaft, in the "wrist" region, while Dcx exhibited a characteristic enrichment along the neurite tip and around the cell body and the two showed overlapping distribution at the wrist (Figure 2A). PP1 showed ubiquitous localization in these neurons, but interaction in a complex with Dcx and Spn was confirmed by coimmunoprecipitation (Figure S2A). We next assessed the distribution of phospho-serine 297 Dcx (PSer297 Dcx) using a phospho-specific antibody (Tanaka et al., 2004b) to the Cdk5 substrate site. PSer297 Dcx showed low but detectable levels in the growth cone but was much reduced in the wrist and the axonal shaft (Figure 2A). Thus Spn was enriched at the wrist, and PSer297 Dcx is largely excluded from axonal shafts, consistent with a model in which Spn/PP1 may mediate dephosphorylation of PSer297 Dcx at the wrist. The close association of the MT-bound Dcx and the actin-bound Spn (Figure 2B) suggested that the Dcx-Spn interaction may serve to coordinate signaling between these cytoskeletal components at the wrist that may in turn be important in axon outgrowth.

## Dcx and Spn Cooperate in Hippocampal Lamination and Corpus Callosum Formation

We next tested for a shared phenotype between the *Dcx* and *Spn* knockout mice, to determine if the two genes share similar roles in brain development. *Dcx* mutant mice display a delamination of the CA3 region of the hippocampus (Corbo et al., 2002). Previous literature indicates a mild reduction in hippocampal size in $Spn^{-/-}$ mice (Feng et al., 2000), so we examined $Spn^{-/-}$ hippocampal anatomy. Surprisingly, 100% of the $Spn^{-/-}$ mice showed a similar mild delamination of the CA3 region (Figure 2C), which was similar in appearance to the $Dcx^{-/y}$ mice. This data suggests that these genes may subserve similar function in brain development.

We next examined the phenotype of P21 mice deficient for both *Dcx* and *Spn*, to determine if there is functional redundancy between these genes during development. Thus we compared $Spn^{-/-}$; $Dcx^{-/y}$ double-knockout (*DKO*) mice with single knockout and WT mice. The hippocampal lamination phenotype was slightly more severe in the *DKO* than was observed in either of the single knockouts (Figure 2C), and there was complete agenesis of the corpus callosum (ACC), which was not observed in either of the single knockouts. The ACC was accompanied by Probst bundles, suggesting failed or delayed axonal extension across the midline during embryogenesis. To determine if this represented a more general disorder of axonal growth, the anatomy of all four genotypes was compared. We noted that the anterior commissure (AC), a major midline decussation tract connecting long-distance reciprocal olfactory and orbital-frontal regions, was hypoplastic in the *DKO* mouse, whereas it appeared normal in both the single knockout mice (Figure 2C). To exclude the possibility that these axonal phenotypes were the result of degeneration rather than failed formation, mice were examined at P0, when these projections have just completed decussation, and stained with the axonal marker L1CAM. We found that the CC decussation was absent even at this age in the *DKO* mouse (Figure 2C). In order to be certain that this phenotype was not due to spontaneous ACC observed in some mouse genetic backgrounds, P0 offspring from twenty litters of $Spn^{+/-}$; $Dcx^{+/-}$ × $Spn^{+/-}$; $Dcx^{+/y}$ matings were analyzed for these phenotypes. From a total of 125 mice, 6 *DKO* mice were identified, 5 of which displayed ACC and hypoplastic AC, whereas none of the 119 mice with intermediate genotypes showed these phenotypes in this genetic background ($p < 0.001$, Figure 2D). This data suggests that Dcx and Spn cooperate to mediate long-distance axonal growth in the CC and AC during development.

## *Spn* and *Dcx* Are Required for MT Bundling in Cortical Neurons

Having established partial functional redundancy between *Dcx* and *Spn* in brain development, we next examined for defects in the actin and MT cytoskeletons in cultured cortical neurons at 1DIV from WT, $Dcx^{-/-}$, $Spn^{-/-}$ and *DKO* littermates. Neurons from all four genotypes were compared in a blinded fashion following visualization of the cytoskeleton. There were no notable differences in actin staining among the four genotypes in either the growth cone or axonal shaft, and MTs were usually observed in close approximation with actin, extending into the growth cone (Figure 3A). However, both $Dcx^{-/-}$ and $Spn^{-/-}$ neurons showed a poorly organized axonal MT cytoskeleton with failure to condense MTs into a single shaft. As a result of splayed and unevenly spaced MTs, axonal shafts were widened compared with WT. Neurons from *DKO* displayed an even broader leading process with apparently more severe failure of MT bundling. This data suggests that the axonal defects may result from impaired MT bundling in the absence of these genes.

## Abnormal Inter-MT Distance in the Absence of Either *Dcx* or *Spn*

To further investigate the ultrastructural basis of this MT phenotype, transmission electron microscopic (TEM) analysis of 1DIV neurons was performed from each of the four genotypes. We noted in WT neurons that MTs were nearly always well organized in the axonal shaft and showed uniform orientation and a typical inter-MT spacing of 20–30 nm (Figure 3B). The neurons from the $Dcx^{-/y}$ and $Spn^{-/-}$ mice, however, showed a disordered MT array. These MTs typically veered in oblique directions within the shaft and showed nonuniform spacing. The neurons from the *DKO* mice appeared even more severely disordered, with frequent MT crossing observed, suggesting a failure of bundling. To quantitate inter-MT distance (IMD), we collected high-resolution images, traced MTs along

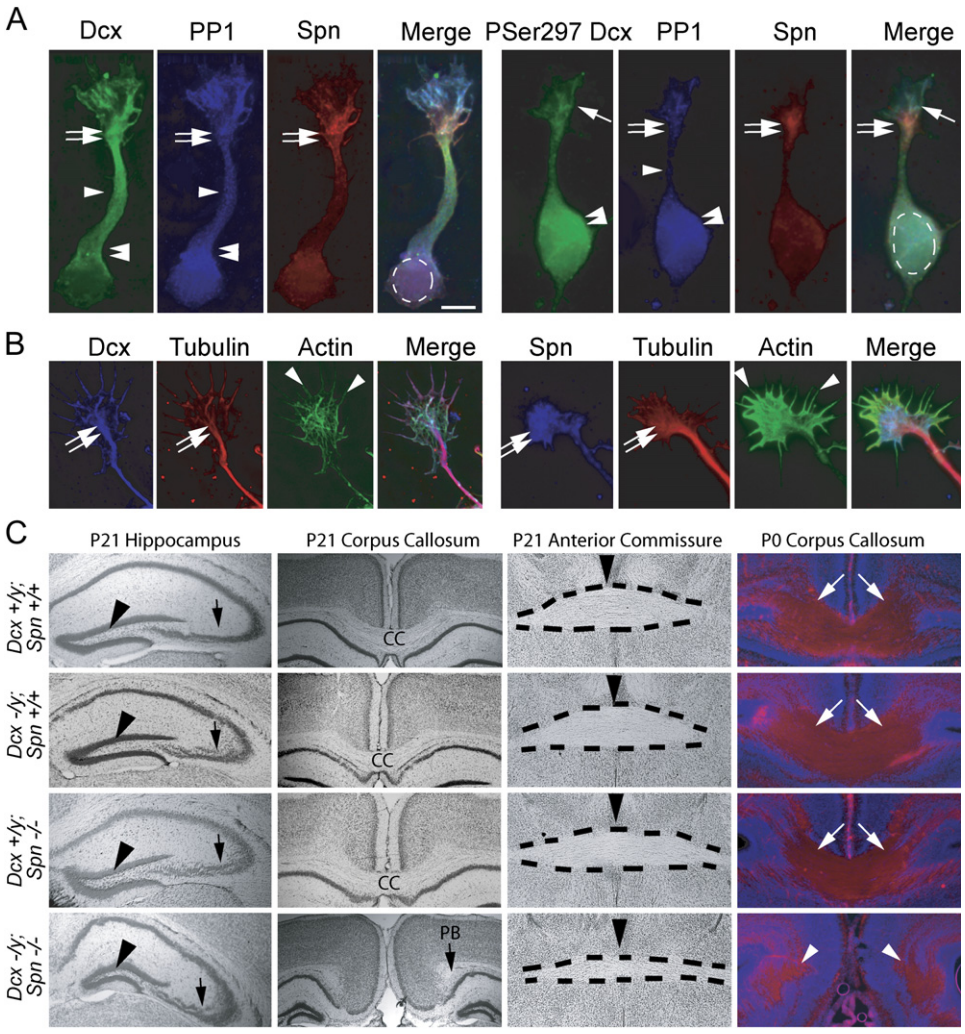


D

| | Genotype | | | | | | | | ⁎ |
|---|---|---|---|---|---|---|---|---|---|
| *Dcx* | +/+ | +/- | -/- | +/+ | +/- | -/- | +/+ | +/- | -/- |
| *Spn* | +/+ | +/+ | +/+ | +/- | +/- | +/- | -/- | -/- | -/- |
| Absent Corpus Callosum Decussation | 0/17 | 0/11 | 0/7 | 0/26 | 0/12 | 0/19 | 0/15 | 0/12 | 5/6 |
| Hypoplastic Anterior Commissure | 0/17 | 0/11 | 0/7 | 0/26 | 0/12 | 0/19 | 0/15 | 0/12 | 5/6 |

**Figure 2. Spn and Dcx Share Protein Distribution and Cofunction during Brain Development**

(A) Dcx exhibited enrichment along MTs at the wrist (double arrows), the axonal shaft (arrowhead), and cell body (double arrowheads), PP1 was distributed diffusely, and Spn was enriched at the wrist (double arrows). PSer297 Dcx had highest expression in the growth cone (arrow) and cell body (double arrowhead). PSer297 Dcx compared with total Dcx was mostly excluded from regions of Spn localization at the wrist (double arrow), suggesting Spn may contribute to its dephosphorylation. The scale bar represents 10 μm.

(B) Dcx and Spn overlap in distribution with the actin and MT cytoskeletons at the wrist (double arrow) and filopodia (arrowheads).

(C) *Dcx* and *Spn* cooperate in axonal outgrowth of multiple long-distance projections. Both $Spn^{-/-}$ and $Dcx^{-/y}$ showed defective lamination of the CA3 region (arrow), whereas $Spn^{-/-}$; $Dcx^{-/y}$ (*DKO*) showed possibly worsened defect compared with single knockouts. The granule cell layer was unaffected (arrowhead). The CC decussation was evident in all but the *DKO*, where it was replaced by Probst bundles (PB). The anterior commissure (dashes) showed normal appearance in all but the *DKO* where it was hypoplastic. Midline indicated by arrowhead. At P0, decussating CC fibers (stained with L1CAM, arrows) were visible in all but the *DKO*, where they terminated in Probst bundles (arrowheads).

(D) Expressivity of ACC and hypoplastic anterior commissure among offspring from 20 litters of double-heterozygous matings. Number of mice with each phenotype over total of each genotype are listed. Note that none of the mice except the $Spn^{-/-}$; $Dcx^{-/-}$ (*DKO*) showed ACC and hypoplastic anterior commissure phenotype. $Dcx^{-/-}$ entries include both −/− females and −/*y* male null mice. * = $p < 0.001$, chi-square test.

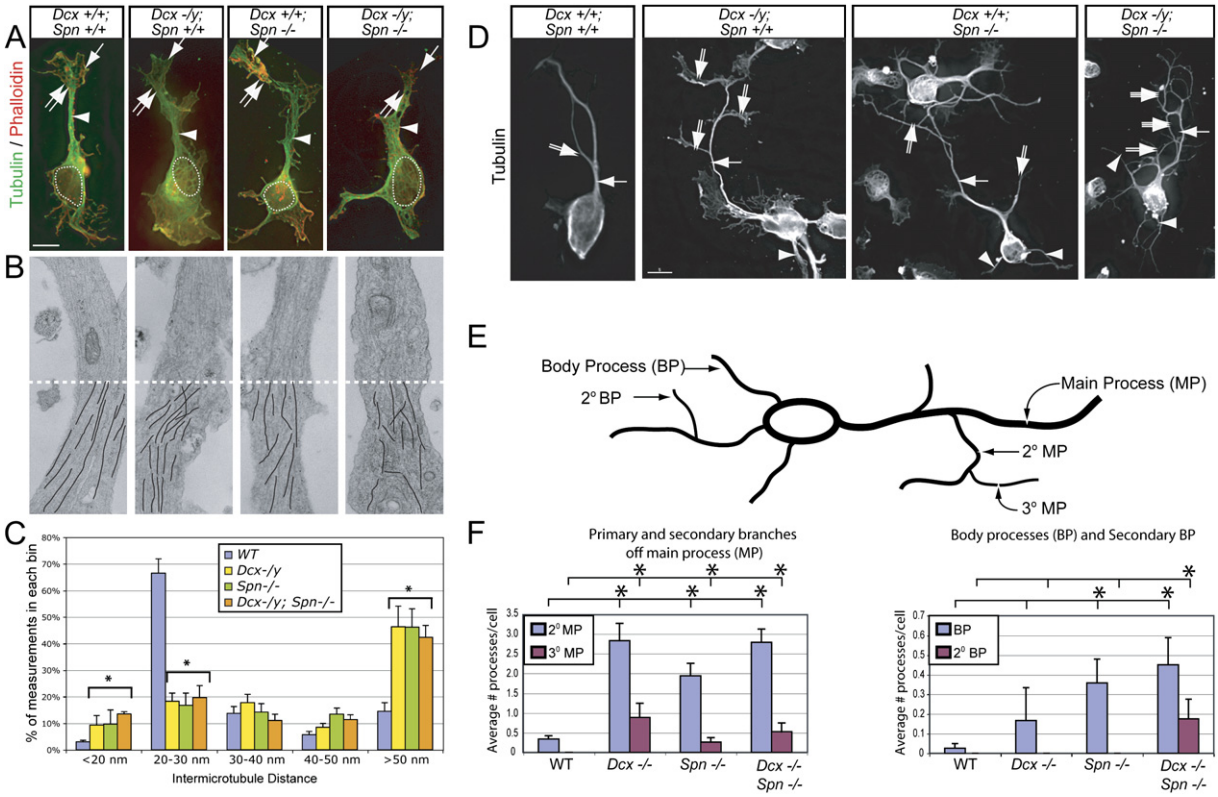


**Figure 3. Disrupted Shaft MT Cytoskeleton in *Dcx*, *Spn*, and *DKO* Mutant Neurons Results in Excessively Branched Neurite Phenotype**

(A) WT showed condensed MTs in the shaft (arrowhead). Wrist (double arrow) and growth cone (arrow) are well-delineated from the cell body (dashed circle = nucleus). In $Dcx^{-/y}$ or $Spn^{-/-}$ neurons, MTs were instead splayed (arrowhead), and as a result, the neurite shaft width was increased.

(B) Transmission electron microscopy showed parallel MT arrays that maintained relatively consistent spacing along the shafts in cultured cortical neurons in WT littermates. This array was disrupted in both single knockouts and was more severe in the *DKO*. Bottom half (dashes) of each shows line tracings depicting MTs. 8000×.

(C) Binned inter-MT distance between nearest neighbor was significantly greater in mutants. n = 1499 total measurements, from 9 WT, 5 $Dcx^{-/-}$, 4 $Spn^{-/-}$, and 5 *DKO* neuronal shafts from two separate culture experiments. * = $p < 0.05$, chi-square contingency table.

(D) WT neurons typically displayed a single monopolar main process (arrow) with occasional 2° branches (double arrow) after 36 hr in culture. Both $Dcx^{-/y}$ and $Spn^{-/y}$ neurons exhibited excessive 2° (double arrows) and 3° (triple arrows) branches from the primary neurite, as well as an increased number of processes extending from the cell soma (arrowhead). This was most striking in *DKO*.

(E) Quantification of neurite branching. Branches from the main process (MP) were termed 2° MP, and branches from 2° MP were termed 3° MP. Neurites extending from the soma were termed body processes (BP), and branches from the BP were termed 2° BP.

(F) WT cells typically had a single MP, with average number of 2° MP per cell less than 0.5. The branching and frequency of 3° MP was increased in $Dcx^{-/y}$, $Spn^{-/-}$ and *DKO* neurons. Furthermore, 2° BP were only noted in *DKO* neurons.

All error bars = SEM. * = $p < 0.05$, pairwise comparison, Student's t test.

their entire visible length and measured nearest neighbor distance at uniform 250 nm intervals along the entire length of the visible neurite from at least 4 neurons of each genotype (for a total of over 300 IMD measurements from each genotype). In WT neurons, there were very few locations where MTs crossed paths, (indicated by an IMD < 20 nm) whereas these were not infrequently encountered in both single knockouts and the *DKO* ($p < 0.05$, Figure 3C). TEM tomography was also performed from cultured neurons from on each of the four genotypes, which showed fragmented and poorly aligned MTs from the single and *DKO* neurons (Movies S1–S5). These results imply a failure to bundle MTs in the absence of *Dcx* and *Spn*.

## Defective MT Bundling Is Associated with Excessively Branched Neurites

Failure to condense neurite MTs often leads to defects in neuronal morphology at later stages of maturation (Szebenyi et al., 1998). To test this, we analyzed morphology of mutant neurons after 36 hr in culture, a time when neurites have typically organized into stable thin processes. Striking defects in morphology were detected in neurons from both single knockouts, with an increase in branching complexity of the main process (MP) as well as an increase in the number branches extending from the cell body (i.e., body processes (BP, Figure 3D). Quantification of the number of 2° and 3° branches from the main process as well as

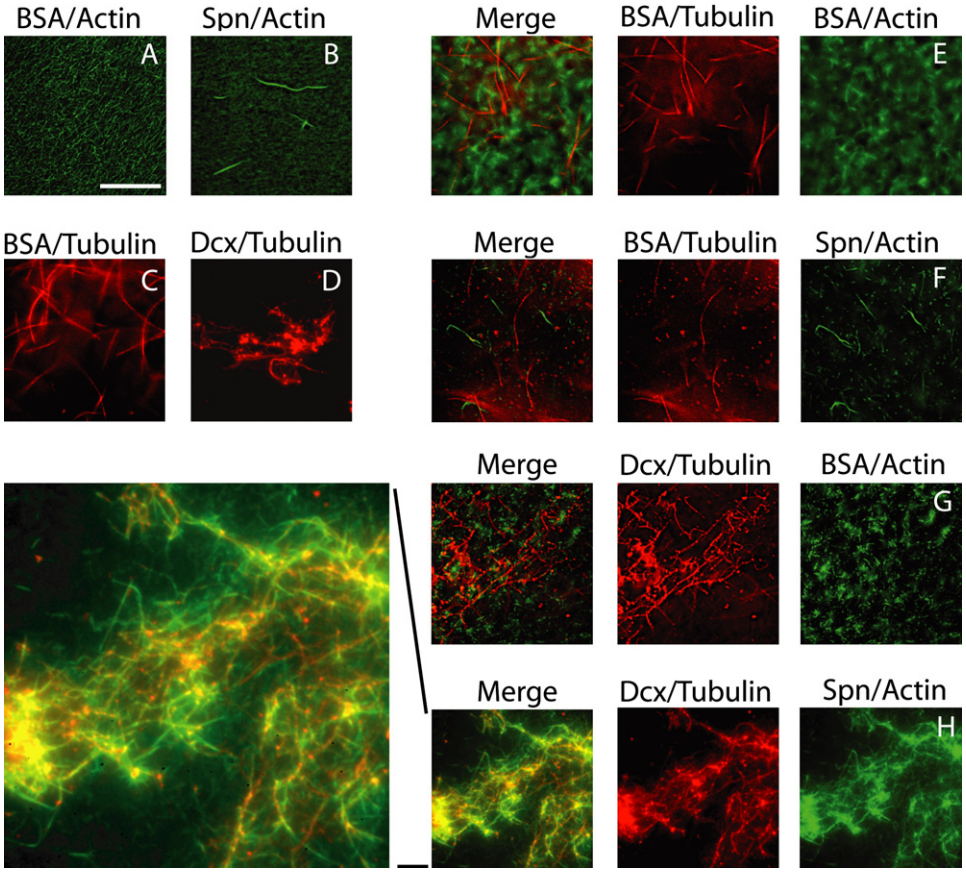


**Figure 4. Dcx/Spn Interaction Sufficient to Corecruit Actin and MT Cytoskeletons**

Purified Spn and Dcx was sufficient to link phalloidin-stabilized actin and taxol-stabilized MTs.

(A and B) Spn added to actin led to production of filaments.

(C and D) Dcx added to tubulin led to asters of MTs.

(E–H) (E) Cytoskeletons alone showed no corecruitment, and neither was tubulin recruited to Spn-stabilized actin (F) or actin recruited to Dcx-stabilized tubulin (G). However, Spn-stabilized actin and Dcx-stabilized MTs showed significant corecruitment of the two cytoskeletons ([H], and higher power view of [H]). Repeated in triplicate.

the number of 1° and 2° body processes performed in a blinded fashion demonstrated statistical evidence of excess of such branches (Figures 3E and 3F). *DKO* neurons showed a further increase in the number of 2° BPs, which were only rarely observed in either WT or $Dcx^{-/-}$ or $Spn^{-/-}$ neurons. We conclude that *Dcx* and *Spn* cooperate for maintenance of neuronal morphology and suppression of excessive branching, which is likely a result of failure to organize the MT cytoskeleton at the wrist.

## Spn and Dcx Interaction Is Sufficient to Crosslink Actin and MTs

We next tested the ability of purified Dcx and Spn to corecruit the actin and MT cytoskeletons in a cell-free assay. Recombinant Spn was added to actin previously polymerized with Alexa 488-labeled phalloidin, resulting in the formation of F-actin filaments (Figure 4). Similarly, rhodamine-conjugated purified tubulin (previously stabilized with a low dose of taxol) was treated with recombinant Dcx, which led to the formation of MT aster-like structures from which MT bundles emanated. The combination of labeled actin and tubulin showed no particular affinity for one another, and neither did the addition of labeled tubulin to Spn-stabilized actin nor did the addition of labeled actin to Dcx-stabilized MTs. However, when Spn-stabilized actin and Dcx-stabilized MTs were combined, there was significant overlap of the two labeled cytoskeletal components. This effect was not merely due to clumping of the two cytoskeletons, because taxol/phalloidin stabilization of these cytoskeletons did not lead to overlap. This data suggests that the Dcx-Spn interaction is sufficient to mediate crosslinking of the actin and MT cytoskeletons in vitro.

## PP1 Is Capable of Mediating Dephosphorylation of PSer297 Dcx

Previous work has established that the kinase Cdk5 is in a complex with the phosphatase PP1 and Spn

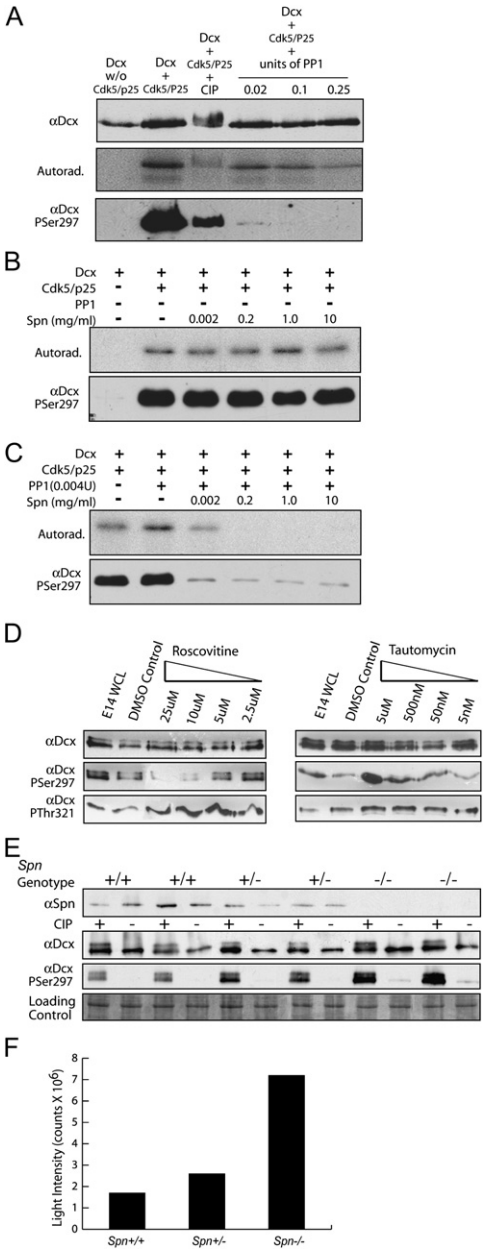


**Figure 5. Spn Required for PP1-Mediated Dephosphorylation of PSer297 Dcx**

(A) PP1 at high unit concentrations was capable of dephosphorylating Dcx at PSer297, based on autoradiogram or immunoreactivity with αPSer297 following [$^{32}$P] incorporation. PP1 was a more specific phosphatase for the PSer297 site than CIP, resulting in nearly complete dephosphorylation at all concentrations tested.

(B) Spn alone has no effect on [$^{32}$P] retention or αPSer297 reactivity.

(C) Low levels of PP1 (5× lower than used in [A]) in the absence of Spn had no effect on [$^{32}$P] retention or αPSer297 reactivity but increasing amounts of Spn promoted dephosphorylation of Dcx by PP1.

(D) PP1 and Cdk5 act in opposing fashions to modulate phosphorylation state of Dcx Ser297 in cortical neurons. Cortical neurons with increasing roscovitine (inhibits Cdk5) or tautomycin (inhibits PP1) were analyzed by Western with Dcx PSer297 and PThr321 antibodies. Roscovitine blocked and tautomycin enhanced PSer297 reactivity but not PThr321.

(E) Brain lysates from E16 littermates showed increased PSer297 reactivity as *Spn* dosage was decreased.

(F) Quantification of PSer297 Dcx band intensity standardized to control shows a 4-fold increase in reactivity in $Spn^{-/-}$ versus $Spn^{+/+}$.

(Agarwal-Mawal and Paudel, 2001), indicating that this complex is well poised to mediate dynamic phosphorylation/dephosphorylation of substrates. We therefore tested whether PP1 was capable of dephosphorylating the Cdk5-mediated phosphorylation of Dcx Ser297. Recombinant Dcx was added to recombinant Cdk5/p25, resulting in robust phosphorylation of Dcx at Ser297 based both on [$^{32}$P] autoradiogram and αPSer297 Dcx reactivity (Figure 5A). The addition of the nonspecific calf intestinal phosphatase (CIP) led to a reduction in both the autoradiogram signal and the reactivity with the αPSer297 Dcx. Increasing concentrations of recombinant PP1 were then compared with CIP for the ability to dephosphorylate this site. We noted a dose-dependent decrease in autoradiogram signal and αPSer297 Dcx reactivity following PP1 treatment. We conclude that PP1 is capable of mediating the dephosphorylation of PSer297 Dcx.

## Spn Enhances PP1-Mediated Dephosphorylation of PSer297 Dcx

Because Spn targets PP1 to phosphoproteins, we next tested whether Spn was capable of enhancing the PP1-mediated dephosphorylation of PSer297 Dcx. The addition of even high concentrations of Spn in the absence of PP1 had no effect on PSer297 Dcx reactivity on Dcx that had been previously phosphorylated with the Cdk5/p25 kinase (Figure 5B). Next, PP1 concentration was reduced to a level where it alone had no effect on the phosphorylation state of Ser297 Dcx (Figure 5C), and then increasing concentrations of Spn were added to this mixture. We noted a Spn dose-dependent dephosphorylation of PSer297 Dcx, which was observed both in autoradiogram and with the PSer297 Dcx antibody. We conclude that Spn is capable of enhancing the PP1-mediated dephosphorylation of PSer297 Dcx.

## Modulation of PSer297-Specific Phosphorylation by Cdk5 and PP1

The previous data suggests that the Spn-PP1 complex is sufficient to mediate dephosphorylation of PSer297 Dcx. Therefore, to address whether it is necessary, we applied membrane-permeable roscovitine, a specific Cdk5 inhibitor (IC50 200 nM, versus >500 nM for cell cycle-related Cdks tested (Meijer et al., 1997)) or tautomycin, a selective PP1 inhibitor (IC50 1nM versus >10 nM for PP2A and other phosphatases (MacKintosh and Klumpp, 1990)) to cultured neurons. Subsequently, cells were lysed and analyzed by Western using a pan-Dcx antibody, a PSer297 Dcx-specific antibody and a PThr321 Dcx-specific antibody, the latter that recognizes a Jun kinase phosphorylation site (Gdalyahu et al., 2004). As roscovitine concentration was increased, there was progressively less reactivity

of the αPSer297 Dcx, without notable change in either total Dcx or PThr321 Dcx reactivity (Figure 5D). Application of tautomycin had the opposite effect, leading to an increase in αPSer297 Dcx reactivity, without change in either the total Dcx or PThr321 Dcx reactivity. We conclude that Cdk5 and PP1 reciprocally regulate the phosphorylation state of Ser297 Dcx.

### PSer297 Dcx Is Excessively Phosphorylated in the Absence of Spn

In order to determine if Spn is necessary for dephosphorylation of PSer297 Dcx, we examined *Spn*$^{-/-}$, *Spn*$^{+/-}$ and *Spn*$^{+/+}$ littermates for αPSer297 Dcx reactivity. Whole brain lysates from E16 littermates were prepared, and CIP was added to half of each sample as a nonspecific phosphatase, and samples were then assayed for Spn, Dcx, and PSer297 Dcx reactivity via Western analysis. We found no notable differences in Dcx levels in any of the genotypes. However, there was dosage-dependent excessive phosphorylation of Ser297 Dcx in the *Spn*$^{+/-}$ and *Spn*$^{-/-}$ brain lysates (Figure 5E). Reactivity was 4-fold higher in the −/− than +/+ brains based on quantitative luminometry (Figure 5F). The data together suggests that Spn-PP1 is necessary and sufficient for PSer297 Dcx dephosphorylation.

### PP1 Function Required for MT Bundling during Neurite Growth

The identification of PP1 as part of the Dcx-Spn complex in brain (Figure S2) prompted us to test PP1's role in MT bundling during neurite outgrowth using genetic knockdown. PP1 consists of two regulatory subunits and a catalytic subunit (PP1γ), that directly associates with Spn (MacMillan et al., 1999). We utilized a previously validated PP1γ siRNA and found a 6-fold reduction in protein expression in culture N2A cells (Figure S3), suggesting that this siRNA mediates robust knockdown of PP1γ expression. Cortical neurons from E13.5 WT mice underwent in utero electroporation with the PP1γ siRNA and marker plasmid, isolated at E14.5, then at 1 DIV were fixed and stained to visualize the MT and actin cytoskeleton. We found that MTs failed to bundle in the majority of PP1γ siRNA expressing cells (Figure 6A). This was quantitated by evaluating the percentage of cells with the phenotype of splayed MT in the primary neurite shaft. We found that approximately 85% of PP1γ electroporated cells showed this phenotype compared with approximately 25% of controls ($p < 0.01$, Figure 6B). We conclude that PP1 catalytic activity is required for bundling of MTs within the leading neurite.

### MT Bundling Depends upon Association of the Dcx-Spn-PP Complex

Because of the shared MT bundling phenotype observed in *Spn* and *Dcx* knockout neurons, we hypothesized that the interaction between these two proteins might be critical for MT bundling in neurites. Because Spn aa L649–Q696 (part of the coiled-coil domain) constituted the consensus Dcx binding domain (Figure S1A), we deleted these residues from Spn (SpnΔCC), and found that this construct failed to coimmunoprecipitate Dcx in cotransfected 293T cells (Figure S1D). Therefore, EGFP-Spn and EGFP-SpnΔCC were tested for their ability to rescue the MT bundling defect in *Spn*$^{-/-}$ neurons. Neurons from E14 *Spn*$^{-/-}$ were electroporated with constructs encoding either plasmid, then at 1DIV were stained for MTs and EGFP, and scored for the bundling defect. The majority of *Spn*$^{-/-}$ neurons with WT Spn showed a normalization of the MT array. However, most neurons electroporated with the SpnΔCC showed persistent MT bundling defects (Figure 6C). Quantification of the number of cells with either bundled or splayed MTs in the leading neurite showed rescue in 78% versus 25% with WT or mutant constructs, respectively (Figure 6D, $p < 0.01$). We conclude that the association between Spn and Dcx is required for MT bundling. The EGFP-Spn4A (residues 457–460 KIKF) mutant construct was similarly tested, which was previously found to lack binding with PP1 (Tsukada et al., 2006), to determine if it was capable of restoring MT bundling in *Spn*$^{-/-}$ neurons. Quantification showed the majority of cells electroporated with EGFP-Spn4A showed similar persistent MT bundling defects (Figures 6C and 6D, $p < 0.01$). We conclude that the interaction between Spn, Dcx and PP1 is important for MT bundling in neurites.

Having demonstrated that the Spn/PP1 complex serves to dephosphorylate PSer297Dcx, we next tested whether Dcx phosphorylation mutants at the 297 site are capable of rescuing the MT cytoskeletal defect in *Dcx*$^{-/y}$ neurons. The Dcx297A mutant is incapable of phosphorylation at this site, whereas the Dcx297D mutant mimics phosphorylation at this site. We found that WT but neither mutant showed a rescue of the splayed MT phenotype (Figure 6E). Quantification of the percentage of cells with either bundled or splayed MTs in the leading neurite showed rescue in 82% versus 19% and 14% with WT, 297A or 297D mutations, respectively (Figure 6F, $p < 0.01$). Together, the data suggest that the interaction of Spn and Dcx as well as the dynamic regulation of the S297 phosphorylation state of Dcx is necessary for maintenance of the MT cytoskeleton during neurite outgrowth.

### Spn-PP1-Mediated Dcx Dephosphorylation Recovers MT Polymerizing Activity

PSer297 Dcx phosphorylation by Cdk5 results in a 60% decrease in MT polymerization activity (Tanaka et al., 2004b), and the data indicates that the Spn-PP1 complex is necessary and sufficient for dephosphorylation at this site. In order to test whether Spn-PP1-mediated PSer297 Dcx dephosphorylation might result in reactivation of its MAP activity, we employed the turbidimetric MT polymerization assay (Gleeson et al., 1999). Application of recombinant Dcx to MAP-depleted brain-derived purified tubulin resulted in robust polymerization (Figure 7A). We then added activated recombinant Cdk5/p25 to phosphorylate Ser297 Dcx, and rezeroed the absorbance reading. There was a subsequent decrease in the turbidity over the following time period, suggesting

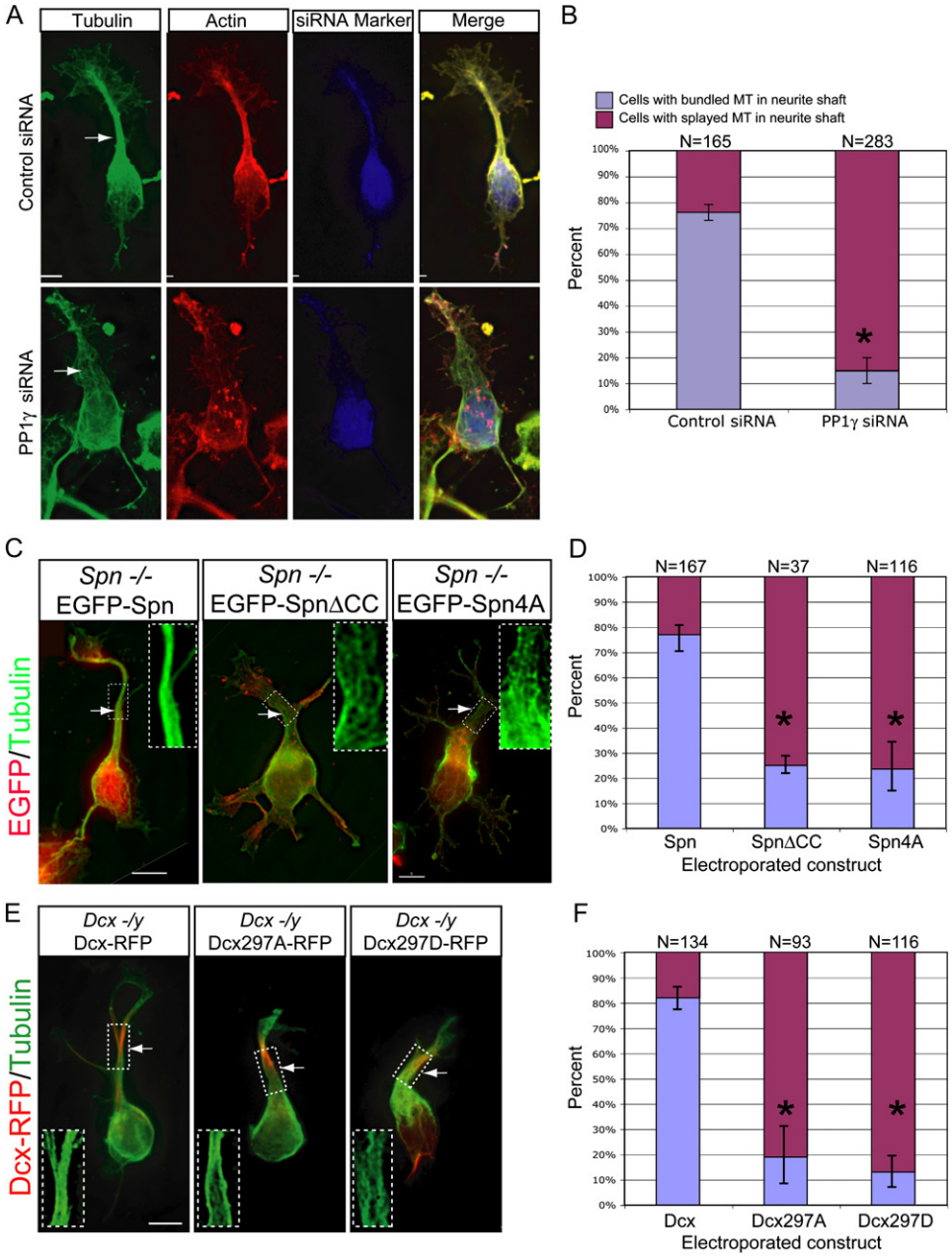


**Figure 6. Spn-PP1-Dcx Complex Required for MT Bundling during Neurite Outgrowth**

(A) PP1γ knockdown associated with failure of MT bundling and broadened primary neurite. (C) *Spn*$^{-/-}$ splayed MT phenotype is rescued by forced expression of EGFP-tagged wild-type Spn, but not SpnΔCC (lacks Dcx binding) or Spn4A (lacks PP1 binding). (E) *Dcx*$^{-/y}$ splayed MT phenotype is rescued by forced expression of Dcx-RFP, but not by Dcx297A (unphosphorylatable) or Dcx297D (pseudophosphorylated) at the Spn-PP1 site. The scale bar represents 5 μm. (B, D, and F) Significant difference in cells with bundled versus splayed MT neurite phenotype. Results averaged from two experiments. All error bars = SEM. * = $p < 0.01$, Student t test.

that phosphorylation of Dcx by Cdk5 results in depolymerization of MTs that had been previously polymerized with Dcx. We then added roscovitine (to inactivate Cdk5), together with recombinant Spn-PP1, to dephosphorylate PSer297 Dcx, and rezeroed the absorbance reading a second time. An increase in the turbidity was once again observed over the following time period, suggesting MT repolymerization as a result of dephosphorylation of the PSer297 Dcx site. We performed two controls for this experiment. In the first, we concurrently added roscovitine together with Cdk5/p25 to the reaction at the beginning of the second incubation to block the kinase activity of

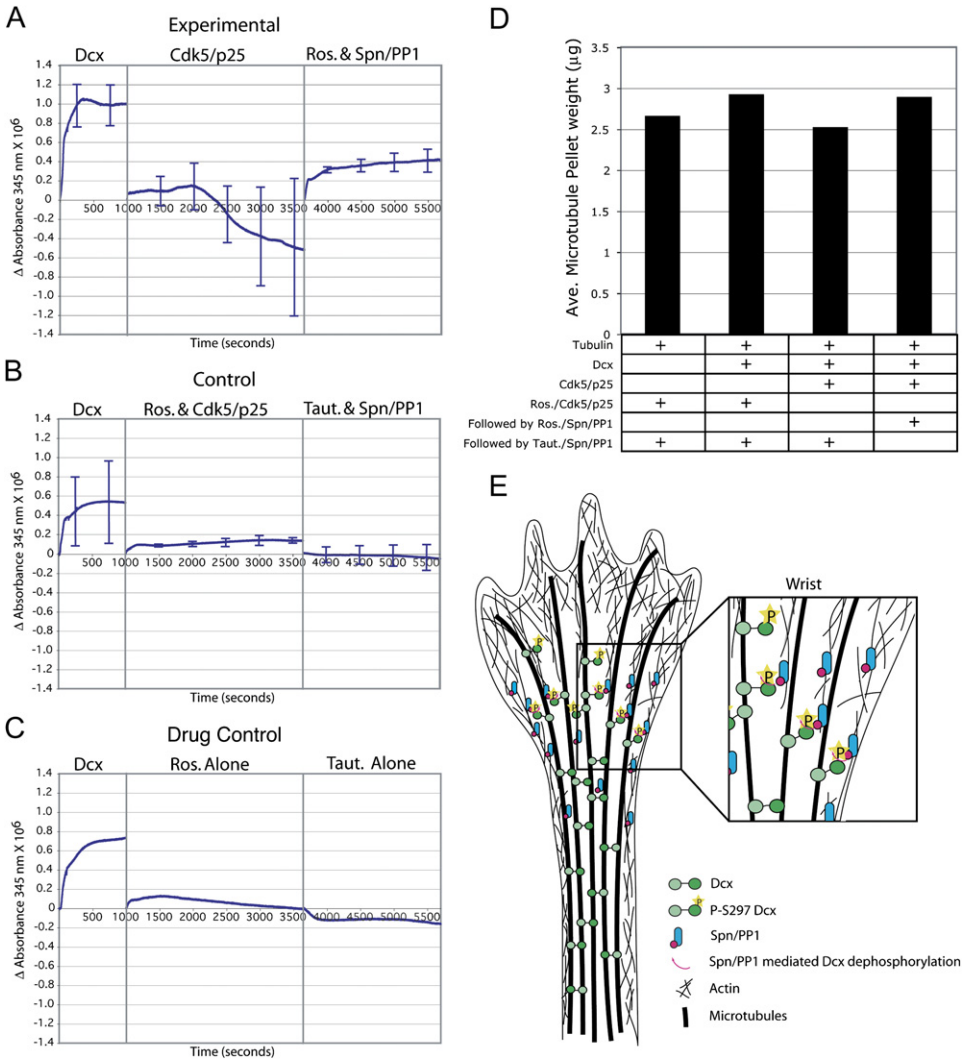


**Figure 7. Spn-PP1-Mediated Dephosphorylation Reinstates the Tubulin Polymerization Effect of Dcx**

(A) Purified Dcx and tubulin shows robust increase in turbidity after 1000 s. Subsequently, addition of activated Cdk5/p25 to phosphorylate Ser297 resulted in a net decrease in turbidity over the next 2500 s. Subsequently, addition of roscovitine (to block Cdk5 activity) and Spn-PP1 (to dephosphorylate PSer297 Dcx) resulted in net increase in turbidity over the next 2500 s.

(B) Cdk5/p25 that was pretreated with roscovitine, or Spn-PP1 that was pretreated with tautomycin had no net effect on turbidity.

(C) Neither roscovitine nor tautomycin alone had any net effect on turbidity. Error bars = SEM from three trials.

(D) Cosedimentation analysis. The dephosphorylation of previously phosphorylated Dcx sites was associated with a reinstatement of Dcx MT polymerizing activity, and associated with an increased MT pellet weight. Averaged from two experiments.

(E) Model for the role of Dcx and Spn in MT organization during neurite extension. Spn is restricted to the wrist region, where it is complexed with PP1. Spn mediates PP1 dephosphorylation of MT-bound PSer 297 Dcx. This leads to reactivation of Dcx, with subsequent MT crosslinking activity that is necessary for MT bundling in the neurite shaft.

Cdk5. This resulted in little change in the overall turbidity of the reaction (Figure 7B). We then added tautomycin concurrently with the Spn-PP1 at the beginning of the third incubation to block the phosphatase activity of PP1. Likewise, this resulted in little change in turbidity. Roscovitine or tautomycin alone resulted in little change in turbidity (Figure 7C).

Turbidity is affected by both MT polymerization and by bundling/cross linking, and thus it was not possible to determine whether these Dcx regulators were altering the organization of MT or leading to depolymerization. To address this, we also performed cosedimentation experiments, to determine the weight of the resultant MT pellet at the end of these experiments. We found that the pellet weight (which correlates to the mass of MTs) showed changes that mirrored turbidity (Figure 7D). The data suggests that dynamic phosphorylation and dephosphorylation can influence the effect of Dcx on MT polymerization.

## DISCUSSION

Here, we present molecular and genetic data that supports a model of MT bundling at the wrist region during neurite extension. In this model, actin-associated Spn at the neurite wrist enhances the PP1-mediated dephosphorylation of Dcx, which reinstates Dcx's microtubule associated activities, allowing the orderly bundling of MTs into the neurite shaft (Figure 7E). This model is supported by data indicating disordered MT bundling along the neurite shaft in *Spn*$^{-/-}$ and *Dcx*$^{-/y}$ cultured neurons. In addition, similar MT disorganization was observed along neurite processes in PP1 siRNA treated cortical neurons. A requirement for Spn in mediating Dcx dephosphorylation at S297 was evident in the increased levels of PSer297 Dcx in the *Spn*$^{-/-}$ brain. MT bundling required the interaction of the Spn/PP1/Dcx complex, as Spn and Dcx expression were capable of rescuing this splayed MT phenotype in respective knockouts, but expression of mutants lacking the ability to form this complex showed failure to rescue the phenotype. This data suggests that Spn is an important adaptor molecule that spatially restricts PP1-mediated Dcx dephosphorylation during neurite outgrowth.

### Genetic Requirements for Corpus Callosal Development

We show delayed axon outgrowth in *Dcx*$^{-/y}$ brains, yet these fibers eventually project to their correct location in a fashion indistinguishable from WT, suggesting a time-dependent defect in axon outgrowth. This delay may enhance the susceptibility of *Dcx*$^{-/y}$ neurons to further genetic perturbations, such as we observed in the *DKO*, and has been previously demonstrated for dosage-dependent interaction with *Dclk1* (Koizumi et al., 2006b) and a strain dependent effect of *Dcx* on CC development (Kappeler et al., 2007). Spn has been shown to interact with both Dcx and Dclk1 (Tsukada et al., 2003), therefore it is possible that the ACC observed in the *DKO* is due to absence of both the Dclk1 or Dcx interaction with Spn. However, since *Spn*$^{-/-}$ alone does not display ACC, it is likely that Dcx has Spn-independent effects on CC development, so that these axons are delayed but reach the midline within the permissive window for decussation (Wahlsten et al., 2006). The combined factors may play a role in the variable expressivity of the ACC phenotype in humans with *Dcx* mutations (Kappeler et al., 2007).

### The Role of Dcx and Spn in Regulation of Neurite Branching

Previous data has suggested a requirement for Dcx in repressing the branching of neurites during migration in both subventricular zone and medial ganglionic eminence neurons (Kappeler et al., 2006; Koizumi et al., 2006a). This excessive branching was reminiscent of what we observed in cultured primary *Dcx*$^{-/-}$ or *Spn*$^{-/-}$ neurons. Branching is typically initiated at the growth cone and along the shaft when MT splay apart, allowing shorter MT to invade the nascent actin-rich branches (Kalil et al., 2000; Szebenyi et al., 1998). It is likely that failure to maintain a bundled MT cytoskeleton in the neurite shaft underlies the excessive branching that we and others have observed.

### Integrators of the Actin and MT Cytoskeleton

Much of the understanding of neurite outgrowth has focused on the role of the actin or MT cytoskeleton independently, and only recently has data emerged to suggest how these two major cytoskeletal components may be coordinated in this process (Dehmelt and Halpain, 2004). This integration is presumably mediated by either single molecules that contain both an actin- and MT-binding domain, or by pairs or complexes of molecules that together contain these domains. Several cellular factors such as Pod-1 contain modular actin and MT binding domains and are themselves capable of crosslinking or integrating the two cytoskeletons (Rothenberg et al., 2003). However, there are few examples of molecular complexes that can *bridge* between these cytoskeletal components. One such example is the IQGAP1/CLIP-170 interaction, in which activated Rac/CDC42 recruits IQGAP1, an actin binding protein, with CLIP-170, a MT plus-end binding protein, to form a tripartite complex for cellular polarization (Fukata et al., 2002).

The current data suggest that the Spn-Dcx interaction may also mediate crosstalk between the actin and MT cytoskeletons. Spn and Dcx display maximal overlap in distribution in the proximal part of the growing neurite tip, at the site of constriction of the neurite that follows the broad growth cone. Dcx has a well-characterized role in MT modulation (Taylor et al., 2000) and Spn not only targets PP1 but is also capable of crosslinking F-actin into bundles (Satoh et al., 1998). In vitro studies have shown Dcx can bridge the actin and MT cytoskeletons independent of Spn (Tsukada et al., 2005). We have also observed that high concentrations of purified Dcx can stabilize and bundle phalloidin labeled actin filaments, however low concentrations of Dcx do not exhibit this effect, but can still crosslink the actin and MT cytoskeletons in combination with Spn. It remains a possibility that Dcx may have Spn-independent interactions with actin in vivo.

### Genetic Evidence of MAP Reactivation through Dephosphorylation

Axonal extension appears to consist of three basic events occurring at the growth cone: protrusion, engorgement, and consolidation (Dent and Gertler, 2003). In this model, protrusion consists of extension of actin-based lamellipodia and filopodia, which then serve as substrates for the extension of MTs. Engorgement consists of movement of vesicles and organelles, likely directed by MT-based transport. Consolidation occurs as the proximal part of the growth cone assumes a cylindrical shape, which probably relies on the bundling of loosely associated MTs. However, little data has been provided to highlight the molecular mechanisms underlying the process. The data presented here suggests that the Dcx/Spn/PP1 interaction may play a role in MT bundling during the consolidation

step. We hypothesize that this effect is part of the molecular machinery involved in the transition from splayed to bundled MTs.

This is the first genetic demonstration to our knowledge of specific adaptor molecules that are required for MAP reactivation. This may be a general mechanism of reactivation of MAPs. Both genetic and pharmacologic evidence support a role for Spn in the PP1-mediated dephosphorylation of Dcx. Spn is capable of enhancing the PP1-mediated dephosphorylation of the PSer297 site of Dcx. *Spn*$^{-/-}$ mice had dramatically increased levels of PSer297 Dcx in developing brain. The phosphatases mediating dephosphorylation of Dcx at other sites are not specifically known, although evidence suggests that PP2A may serve to regulate the phosphorylation state of Ser47 (Schaar et al., 2004). Further identification of the specific phosphatases and targeting subunits for Dcx and other MAPs will require both biochemical and genetic evidence.

## EXPERIMENTAL PROCEDURES

### Kinase/Phosphatase Assay

Proteins were concentrated to 2 mg/ml and used as described (Niethammer et al., 2000; Taylor et al., 2000). Spn, PP1 (Upstate), and Dcx kinase reaction were incubated for 45 min at 37°C in PP1 buffer.

### Animals

*Spn* animals were maintained in a mixed SvJ/129 background. *Dcx* animals were maintained on a mixed 129/BlSwiss background. Animal work was performed on littermates, and was carried out in compliance with Institutional Animal Care and Use Committee approved protocols. Approximately 0.2 μl of DiI (10% in DMF) was injected into the medial subcortical region, and processed for visualization after 2 weeks.

### Cortical Cultures

Cortical neurons were isolated and cultured as described (Zaman et al., 1999). Tautomycin and Roscovitine (Calbiochem) were applied for 2 hr.

### Electroporation

Isolated cortical neurons from littermates were electroporated with a Nucleofector kit performed according to Mouse Neuron protocol (Amaxa Inc.) with full-length pcDNA3 encoding Spn-GFP or SpnΔCC (ΔL649-Q696), or pcDNA3.1 encoding Dcx-RFP with specific mutations (Tanaka et al., 2004b). E13.5 intraventricular injection of PP1γ siRNA (20uM, SCBT) with 1 μg/μl pGE2hrGFP (electroporation marker) or other tagged constructs, with 0.01% Fast Green (USB, injection marker) was performed as described (Tabata and Nakajima, 2001) using 7 mm tweezertrods (Harvard Apparatus). Cortical cultures were generated 48hr post electroporation.

### Microscopy

Fluorescent microscopy was performed essentially as described (Tanaka et al., 2004a). We used rabbit anti-Spn (1:200, Upstate), mouse anti-PP1 (1:50, SCBT), rabbit anti-Dcx (1:200, SCBT), rabbit anti-PSer297 Dcx (1:50), rat anti-L1 (1:200, Chemicon). A branched process was defined as longer than the diameter of the cell body and was more than one cell-body distance from the tip of the main process (to differentiate these from branched growth cone). Electron microscopy was performed using a standard protocol (Yu and Baas, 1994), sectioned at 80 nM, stained with Sato's lead solution, and captured on a JEM-4000EX IV system. Inter MT distances were measured every 250 nm along the visible process length, with contingency table analysis used for statistics.

### Actin/MT Crosslinking Assay

Crosslinking was performed as described (Rothenberg et al., 2003). Lyophylized actin was resuspended in 10× KMEI buffer to 0.4 mg/ml, and stabilized with 60 nM Alexa 488-phalloidin. Rhodamine-tubulin:PCP tubulin (1:10) was diluted to 1 mg/ml in BRB80 with 0.5 μM taxol. Crosslinking was tested by combining actin and MT in combinations of 0.75 mg/ml BSA, recombinant Dcx or Spn for 10 min, fixing in 0.1% glutaraldehyde/20% glycerol prior to imaging.

### MT Turbidity and Cosedimentation Assay

MT polymerization assays were performed as previously described (Gleeson et al., 1999; Taylor et al., 2000). After 10 min 3 μg of recombinant Cdk5/p25 and 50 μM ATP were added to the Dcx reaction and diffraction was zeroed. The reaction was allowed to proceed for 43 min at which time 100 μM roscovitine, recombinant Spn (0.1 μg) and 0.001 units of PP1 were added. Diffraction was zeroed and the turbidity was recorded for an additional 35 min. Tautomycin was used at 10 nM.

PCP-purified tubulin (100 μg) was incubated with recombinant Dcx (10 μg) that was pretreated with 5 μg active or inactive (100 μM roscovitine) Cdk5/p25 (30 min at 37°C) followed by 0.1 μg/0.001units active or inactive (10 nM tautomycin) Spn/PP1 (20 min 37°C). The100 μl reaction containing 1× G-PEM (80 mM Na Pipes, 0.5 mM $MgCl_2$, 1.0 mM EGTA, 1 mM GTP [pH 6.8]) and kinase buffer were pelleted at 37,000 rpm for 20 min at 37°C. The pellets were dried at room temperature for 5 min before weighting.

### Supplemental Data

Supplemental Data include Supplemental Experimental Procedures, Supplemental References, three figures, and five movies and can be found with this article online at http://www.cell.com/cgi/content/full/129/3/579/DC1/.

## ACKNOWLEDGMENTS

We wish to thank Anthony Wynshaw-Boris and Christopher Walsh for the *Dcx* knockout mouse; O. Reiner for the PThr321 Dcx antibody; G. Eichle and A. Proksch for the Spn4A construct; R. Tsien for shared equipment; W. Dobyns for MRI expertise; and the UCSD Neuroscience Microscopy Imaging Core for imaging advice. K. Siever and Y. Fang contributed expertise. We thank J. Dixon, D. O'Leary, A. Ghosh, R. Firtel, B. Zheng, and anonymous reviewers for suggestions. This work was supported by the UCSD Genetics Training grant (to S.L.B.), the Searle Scholars, the Merck Award in Developmental Disabilities, the NINDS (to J.G.G.), and NIH grants P41 RR04050 and R01 NS14718 (to M.H.E.).

Received: August 30, 2006
Revised: December 13, 2006
Accepted: March 13, 2007
Published: May 3, 2007

## REFERENCES

Agarwal-Mawal, A., and Paudel, H.K. (2001). Neuronal Cdc2-like protein kinase (Cdk5/p25) is associated with protein phosphatase 1 and phosphorylates inhibitor-2. J. Biol. Chem. *276*, 23712–23718.

Allen, P.B., Ouimet, C.C., and Greengard, P. (1997). Spinophilin, a novel protein phosphatase 1 binding protein localized to dendritic spines. Proc. Natl. Acad. Sci. USA *94*, 9956–9961.

Arlotta, P., Molyneaux, B.J., Chen, J., Inoue, J., Kominami, R., and Macklis, J.D. (2005). Neuronal subtype-specific genes that control corticospinal motor neuron development in vivo. Neuron *45*, 207–221.

Ceulemans, H., and Bollen, M. (2004). Functional diversity of protein phosphatase-1, a cellular economizer and reset button. Physiol. Rev. *84*, 1–39.

Corbo, J.C., Deuel, T.A., Long, J.M., LaPorte, P., Tsai, E., Wynshaw-Boris, A., and Walsh, C.A. (2002). Doublecortin is required in mice for lamination of the hippocampus but not the neocortex. J. Neurosci. *22*, 7548–7557.

Dehmelt, L., and Halpain, S. (2004). Actin and microtubules in neurite initiation: are MAPs the missing link? J. Neurobiol. *58*, 18–33.

Dent, E.W., and Gertler, F.B. (2003). Cytoskeletal dynamics and transport in growth cone motility and axon guidance. Neuron *40*, 209–227.

des Portes, V., Pinard, J.M., Billuart, P., Vinet, M.C., Koulakoff, A., Carrie, A., Gelot, A., Dupuis, E., Motte, J., Berwald-Netter, Y., et al. (1998). A novel CNS gene required for neuronal migration and involved in X-linked subcortical laminar heterotopia and lissencephaly syndrome. Cell *92*, 51–61.

Feng, J., Yan, Z., Ferreira, A., Tomizawa, K., Liauw, J.A., Zhuo, M., Allen, P.B., Ouimet, C.C., and Greengard, P. (2000). Spinophilin regulates the formation and function of dendritic spines. Proc. Natl. Acad. Sci. USA *97*, 9287–9292.

Friocourt, G., Koulakoff, A., Chafey, P., Boucher, D., Fauchereau, F., Chelly, J., and Francis, F. (2003). Doublecortin functions at the extremities of growing neuronal processes. Cereb. Cortex *13*, 620–626.

Fukata, M., Watanabe, T., Noritake, J., Nakagawa, M., Yamaga, M., Kuroda, S., Matsuura, Y., Iwamatsu, A., Perez, F., and Kaibuchi, K. (2002). Rac1 and Cdc42 capture microtubules through IQGAP1 and CLIP-170. Cell *109*, 873–885.

Gdalyahu, A., Ghosh, I., Levy, T., Sapir, T., Sapoznik, S., Fishler, Y., Azoulai, D., and Reiner, O. (2004). DCX, a new mediator of the JNK pathway. EMBO J. *23*, 823–832.

Gleeson, J.G., Lin, P.T., Flanagan, L.A., and Walsh, C.A. (1999). Doublecortin is a microtubule-associated protein and is expressed widely by migrating neurons. Neuron *23*, 257–271.

Kalil, K., Szebenyi, G., and Dent, E.W. (2000). Common mechanisms underlying growth cone guidance and axon branching. J. Neurobiol. *44*, 145–158.

Kappeler, C., Dhenain, M., Phan Dinh Tuy, F., Saillour, Y., Marty, S., Fallet-Bianco, C., Souville, I., Souil, E., Pinard, J.M., Meyer, G., et al. (2007). Magnetic resonance imaging and histological studies of corpus callosal and hippocampal abnormalities linked to doublecortin deficiency. J. Comp. Neurol. *500*, 239–254.

Kappeler, C., Saillour, Y., Baudoin, J.P., Tuy, F.P., Alvarez, C., Houbron, C., Gaspar, P., Hamard, G., Chelly, J., Metin, C., and Francis, F. (2006). Branching and nucleokinesis defects in migrating interneurons derived from doublecortin knockout mice. Hum. Mol. Genet. *15*, 1387–1400.

Koizumi, H., Higginbotham, H., Poon, T., Tanaka, T., Brinkman, B.C., and Gleeson, J.G. (2006a). Doublecortin maintains bipolar shape and nuclear translocation during migration in the adult forebrain. Nat. Neurosci. *9*, 779–786.

Koizumi, H., Tanaka, T., and Gleeson, J.G. (2006b). Doublecortin-like kinase functions with doublecortin to mediate fiber tract decussation and neuronal migration. Neuron *49*, 55–66.

MacKintosh, C., and Klumpp, S. (1990). Tautomycin from the bacterium Streptomyces verticillatus. Another potent and specific inhibitor of protein phosphatases 1 and 2A. FEBS Lett. *277*, 137–140.

MacMillan, L.B., Bass, M.A., Cheng, N., Howard, E.F., Tamura, M., Strack, S., Wadzinski, B.E., and Colbran, R.J. (1999). Brain actin-associated protein phosphatase 1 holoenzymes containing spinophilin, neurabin, and selected catalytic subunit isoforms. J. Biol. Chem. *274*, 35845–35854.

Meijer, L., Borgne, A., Mulner, O., Chong, J.P., Blow, J.J., Inagaki, N., Inagaki, M., Delcros, J.G., and Moulinoux, J.P. (1997). Biochemical and cellular effects of roscovitine, a potent and selective inhibitor of the cyclin-dependent kinases cdc2, cdk2 and cdk5. Eur. J. Biochem. *243*, 527–536.

Niethammer, M., Smith, D.S., Ayala, R., Peng, J., Ko, J., Lee, M.S., Morabito, M., and Tsai, L.H. (2000). NUDEL is a novel Cdk5 substrate that associates with LIS1 and cytoplasmic dynein. Neuron *28*, 697–711.

Ohshima, T., Ward, J.M., Huh, C.G., Longenecker, G., Veeranna, Pant, H.C., Brady, R.O., Martin, L.J., and Kulkarni, A.B. (1996). Targeted disruption of the cyclin-dependent kinase 5 gene results in abnormal corticogenesis, neuronal pathology and perinatal death. Proc. Natl. Acad. Sci. USA *93*, 11173–11178.

Ramón y Cajal, S. (1988). Cajal on the cerebral cortex: An annotated translation of the complete writings (New York: Oxford University Press).

Rothenberg, M.E., Rogers, S.L., Vale, R.D., Jan, L.Y., and Jan, Y.N. (2003). Drosophila pod-1 crosslinks both actin and microtubules and controls the targeting of axons. Neuron *39*, 779–791.

Satoh, A., Nakanishi, H., Obaishi, H., Wada, M., Takahashi, K., Satoh, K., Hirao, K., Nishioka, H., Hata, Y., Mizoguchi, A., and Takai, Y. (1998). Neurabin-II/spinophilin. An actin filament-binding protein with one pdz domain localized at cadherin-based cell-cell adhesion sites. J. Biol. Chem. *273*, 3470–3475.

Schaar, B.T., Kinoshita, K., and McConnell, S.K. (2004). Doublecortin microtubule affinity is regulated by a balance of kinase and phosphatase activity at the leading edge of migrating neurons. Neuron *41*, 203–213.

Szebenyi, G., Callaway, J.L., Dent, E.W., and Kalil, K. (1998). Interstitial branches develop from active regions of the axon demarcated by the primary growth cone during pausing behaviors. J. Neurosci. *18*, 7930–7940.

Tabata, H., and Nakajima, K. (2001). Efficient in utero gene transfer system to the developing mouse brain using electroporation: visualization of neuronal migration in the developing cortex. Neuroscience *103*, 865–872.

Tanaka, T., Serneo, F.F., Higgins, C., Gambello, M.J., Wynshaw-Boris, A., and Gleeson, J.G. (2004a). Lis1 and doublecortin function with dynein to mediate coupling of the nucleus to the centrosome in neuronal migration. J. Cell Biol. *165*, 709–721.

Tanaka, T., Serneo, F.F., Tseng, H.C., Kulkarni, A.B., Tsai, L.H., and Gleeson, J.G. (2004b). Cdk5 phosphorylation of doublecortin ser297 regulates its effect on neuronal migration. Neuron *41*, 215–227.

Taylor, K.R., Holzer, A.K., Bazan, J.F., Walsh, C.A., and Gleeson, J.G. (2000). Patient mutations in doublecortin define a repeated tubulin-binding domain. J. Biol. Chem. *275*, 34442–34450.

Tsukada, M., Prokscha, A., and Eichele, G. (2006). Neurabin II mediates doublecortin-dephosphorylation on actin filaments. Biochem. Biophys. Res. Commun. *343*, 839–847.

Tsukada, M., Prokscha, A., Oldekamp, J., and Eichele, G. (2003). Identification of neurabin II as a novel doublecortin interacting protein. Mech. Dev. *120*, 1033–1043.

Tsukada, M., Prokscha, A., Ungewickell, E., and Eichele, G. (2005). Doublecortin association with actin filaments is regulated by neurabin II. J. Biol. Chem. *280*, 11361–11368.

Wahlsten, D., Bishop, K.M., and Ozaki, H.S. (2006). Recombinant inbreeding in mice reveals thresholds in embryonic corpus callosum development. Genes Brain Behav. *5*, 170–188.

Yu, W., and Baas, P.W. (1994). Changes in microtubule number and length during axon differentiation. J. Neurosci. *14*, 2818–2829.

Zaman, K., Ryu, H., Hall, D., O'Donovan, K., Lin, K.I., Miller, M.P., Marquis, J.C., Baraban, J.M., Semenza, G.L., and Ratan, R.R. (1999). Protection from oxidative stress-induced apoptosis in cortical neuronal cultures by iron chelators is associated with enhanced DNA binding of hypoxia-inducible factor-1 and ATF-1/CREB and increased expression of glycolytic enzymes, p21(waf1/cip1), and erythropoietin. J. Neurosci. *19*, 9821–9830.